

Surface induced atomic scale demixing in BiSn eutectic alloy

Oleg G. Shpyrko,^{1,*} Alexei Yu. Grigoriev,¹ Reinhard Streitel,¹
Diego Pontoni,¹ Peter S. Pershan,¹ Moshe Deutsch,² and Ben Ocko³

¹*Department of Physics and Division of Engineering and Applied Sciences,
Harvard University, Cambridge MA 02138 (USA)*

²*Department of Physics, Bar-Ilan University, Ramat-Gan 52900 (Israel)*

³*Department of Physics, Brookhaven National Lab, Upton NY 11973 (USA)*

(Dated: February 15, 2019)

Resonant x-ray reflectivity measurements of eutectic $\text{Bi}_{43}\text{Sn}_{57}$ alloy surface reveal atomic-scale demixing extending over three near-surface atomic layers. Nearly complete Bi segregation within the surface monolayer agrees well with Gibbs adsorption theorem. We further show that the observed demixing is consistent with Prigogine-Defay adsorption theory, assuming that Bi-Sn attractive pairing interactions at the surface dominate entropy contributions.

PACS numbers: 68.10.-m, 61.10.-i

One of the earliest theories of surface thermodynamics is that of the so-called *Gibbs adsorption* described in 1878 seminal work by Gibbs [1]: the lower surface energy component of a binary mixture is expected to segregate at the surface. Metallic liquids are ideal systems for studying Gibbs adsorption due to the nearly spherical shape of interacting particles, relative simplicity and the short range nature of interactions and a well-developed knowledge of bulk thermodynamics for many binary alloys. While certain aspects of Gibbs theory can be tested through macroscopic measurement of surface tension or adsorption isotherms, there has been relatively few studies of atomic-scale composition profiles of the liquid-vapor interface. In addition to fundamental questions related to surface thermodynamics of binary liquids, multi-component low melting temperature alloys based on BiSn have gained tremendous amount of attention as substitutes for toxic Pb-based solders [2] resulting in increased interest in their wetting, spreading, alloying, reactivity and other surface-related properties. Furthermore, behavior of alloy-based nanoscale materials is expected to be governed primarily by such interfacial phenomena, as demonstrated recently in studies of liquid-solid phase stability of nanometer-sized BiSn particles [3].

Application of synchrotron radiation techniques make it possible to determine surface structure of liquids with an Ångström-scale resolution that is currently unmatched by any other surface technique. These developments resulted in discovery of *surface-induced atomic layering*: quasi-crystalline ordering of atoms at the liquid-vapor interface into surface-parallel layers. Layering has been experimentally observed in a number of elemental metallic liquids [4, 5, 6, 7, 8] and binary alloys, while it appears to be absent in water [9]. Resonant x-ray reflectivity techniques have been successfully applied to GaIn [10], HgAu [11] and BiIn [12] binary alloys. These measurements produced detailed element-specific composition profiles of the surface, revealing adsorption amount

in the uppermost surface monolayer, while composition of subsequent layers was found to be equal to that of the bulk, in accordance with Gibbs theory. Such observations are in stark contrast with the present study which finds evidence of atomic-scale phase separation extending over at least three atomic layers. Results reported here are somewhat unexpected due to the eutectic nature and nearly perfect solution behavior of $\text{Bi}_{43}\text{Sn}_{57}$ alloy.

Liquid $\text{Bi}_{43}\text{Sn}_{57}$ sample (99.99% purity, Alfa Aesar) was prepared in UHV conditions ($P < 10^{-9}$ Torr). Atomically clean liquid surface was prepared through a combination of mechanical scraping and subsequent Ar^+ ion sputtering. UHV chamber and sample preparation procedures have been described by us previously [7, 13, 14]. Measurements were performed at the liquid surface diffractometer facility of the ChemMatCARS beamline, Advanced Photon Source, Argonne National Laboratory, Argonne IL. During the experiment sample temperature was kept at $T = 142$ °C, 4 degrees above the eutectic temperature of $\text{Bi}_{43}\text{Sn}_{57}$ alloy, 138 °C. Detailed descriptions of x-ray resonant reflectivity technique used in this study can be found elsewhere [12, 14]. X-ray reflectivity $R(q_z)$ deviates from classical Fresnel behavior $R_F(q_z)$ by a square of surface structure factor $\Phi(q_z)$ convolved with contributions from thermal capillary wave fluctuations, $CW(q_z)$:

$$R(q_z) = R_F(q_z) \cdot |\Phi(q_z)|^2 \otimes CW(q_z) \quad (1)$$

Surface structure factor $\Phi(q_z)$ is directly related to intrinsic electron density profile across the liquid-vapor interface, $\rho(e)$:

$$\Phi(q_z) = \frac{1}{\rho_\infty} \int dz \frac{d\langle \rho(z) \rangle}{dz} \exp(iq_z z) \quad (2)$$

where ρ_∞ is taken to be the electron density of the bulk. Detailed analysis of capillary wave contributions $CW(q_z)$ allows separation of thermal effects resulting in unequivocal determination of $\Phi(q_z)$ and subsequently $\rho(e)$ [7, 9].

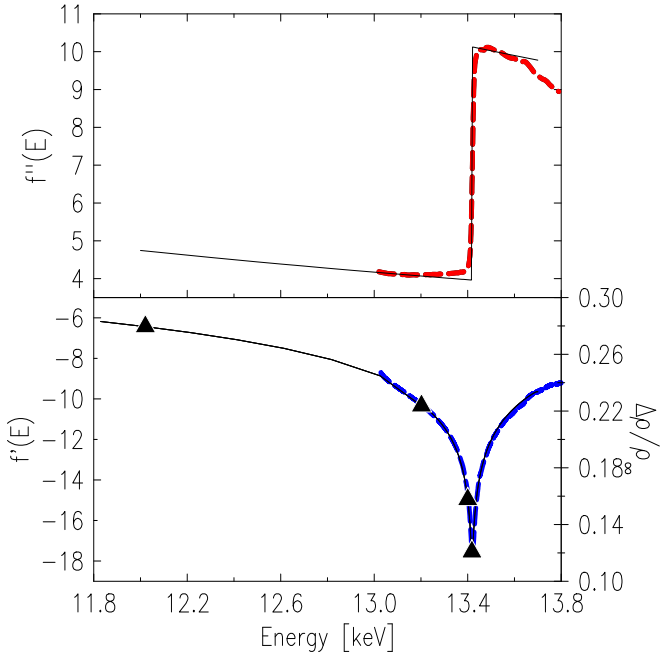


FIG. 1: Atomic scattering factors $f'(E)$ (solid black line theory and dashed blue line experiment) and $f''(E)$ (solid black line theory and dashed red line experiment) for Bi near the L3 absorption edge $E=13.418$ keV. Right scale of lower inset represents electron density contrast $\Delta\rho/\rho_\infty$ converted from $f'(E)$. Triangles mark the energies at which x-ray reflectivities were taken: 12.00 keV, 13.20 keV, 13.40 keV, and 13.42 keV.

Element-sensitive composition profile can be determined from resonant measurements since effective electron density involved in scattering is a strong function of x-ray energy near the adsorption edge of a specific element:

$$\rho_e \simeq (Z + f'(E))\rho_a \quad (3)$$

Here Z is the atomic number, $f'(E)$ is the atomic scattering form factor, while ρ_a and ρ_e are atomic and effective electron densities, respectively. We have measured scattering factor $f''(E)$ in the vicinity of Bi L3 edge $E=13.418$ keV by x-ray absorption through Bi foil, shown along with theoretically calculated $f''(E)$ [15] in the upper inset of Fig. 1. Experimental $f''(E)$ data were then converted to $f'(E)$ through numerical integration of Kramers-Kronig relation [16], compared to theoretical simulations [17] in the lower inset of Fig. 1. Relying on experimentally obtained $f'(E)$ dependence we can determine the composition dependence of the electron density profile described by the distorted crystal model [4]:

$$\frac{\langle \rho(z) \rangle}{\rho_\infty} = \sum_{n=1}^{\infty} \frac{d \exp[-(z - nd)^2/\sigma_n^2]}{\sqrt{2\pi}\sigma_n} \left(1 + \delta_n \frac{\Delta\rho}{\rho_\infty} \right) \quad (4)$$

where $\sigma_n^2 = \sigma_0^2 + (n-1)\bar{\sigma}^2$ describes gradual increase of width for layer n to account for layering decay, $\delta_n =$

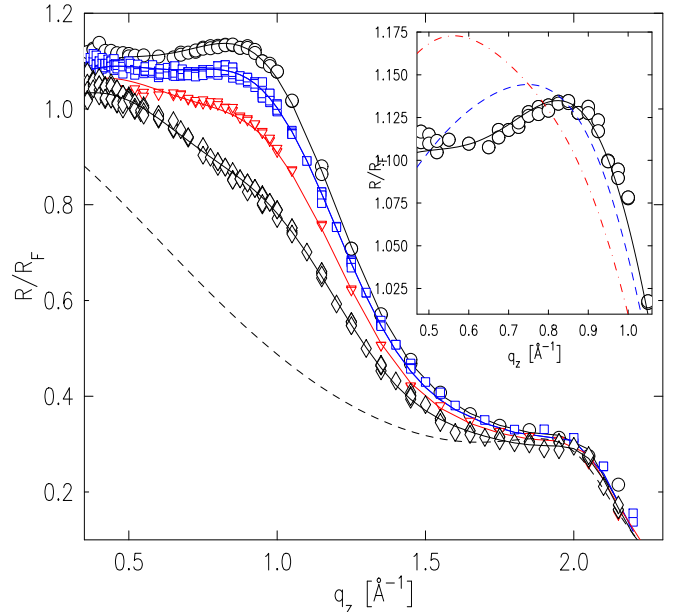


FIG. 2: X-ray reflectivities taken at $E=12.00$ keV (circles), 13.20 keV (boxes), 13.40 keV (triangles) and 13.42 keV (diamonds). Solid lines represent three-layer adsorption model, while dashed line is simulated reflectivity assuming equal composition in all atomic layers. The insets compares $E=12.00$ keV data in the low- q_z region with the least-squared fits to three-layer model (solid black line), two-layer model (dashed blue line) and one-layer model (dashed-dotted red line). Statistical error bars are smaller than the size of the symbols. For explanation of different models see text

$x_n - x$ is the difference between composition of species A in n -th layer x_n and that of the bulk x , while $\Delta\rho = \rho_A - \rho_B$ is the effective electron density difference between species A and B. Density contrast $\Delta\rho(E)/\rho_\infty(E)$ for $\text{Bi}_{43}\text{Sn}_{57}$ alloy converted from $f'(E)$ measurements varies from 0.28 at $E=12.00$ keV to 0.12 at $E=13.418$ keV (see right axis scale of Fig. 1). This energy dependence allows detailed determination of δ_n from resonant reflectivity measurements. Fig. 2 shows Fresnel-normalized reflectivity $R(q_z)/R_F(q_z)$ taken in the vicinity of Bi L3 edge at four selected x-ray energy values marked with triangles in Fig. 1. Surface layering peak is clearly visible at $q_z = 2.0 \text{ \AA}^{-1}$ while the secondary peak at $q_z \simeq 1.0 \text{ \AA}^{-1}$ arises from composition fluctuations between adjacent surface layers. Dashed line corresponds to the simulated $R(q_z)/R_F(q_z)$ assuming all layers have the same composition ($\delta_n = 0$). Strong enhancement over regular layering model and energy-dependence of reflectivity data in the low- q_z region is a clear indication of a significant enhancement of Bi at the surface. We have attempted three approaches to fitting the data using the distorted crystal density model described in Eq. 4. Our first model assumed that only the surface monolayer has a composition different from the bulk, i.e. $\delta_1 \neq 0$, while $\delta_{n \geq 2} = 0$. The second approach extended composition variations to

the first two layers, i.e. $\delta_{1,2} \neq 0$, while $\delta_{n \geq 3} = 0$. Our third model used the compositions of the first three layers as adjustable parameters (fitting $\delta_{1,2,3} \neq 0$, while keeping $\delta_{n \geq 4} = 0$). Layering parameters used for all three of the described models were $d = 2.90 \text{ \AA}$, $\sigma_0 = 0.30 \text{ \AA}$ and $\bar{\sigma} = 0.57 \text{ \AA}$ as determined from the position, shape and intensity of the surface layering peak. Least-squared fitting analysis was performed for four energy data sets simultaneously using experimentally determined $f'(E)$. Table I contains experimental x_n and $\delta_n^E = x_n - x$ values used in three-layer model along with corresponding 95% non-linear confidence intervals $Y(x_n)$ and $Y(\delta_n^E)$ determined from a six-parameter support plane analysis [18]. As can be seen from Fig. 2 three-layer model (represented by solid lines) agrees with the data exceptionally well, while one-layer and two-layer adsorption models do not (see inset of Fig. 2). One of the most striking results is that the deviation of Bi composition from 43% bulk value fluctuates between Bi excess in the first layer (92%), depletion in the second layer (24%) and slight excess in the third layer (53%). These fluctuations asymptotically approach bulk composition for each subsequent subsurface layer as the diminishing residual effects of surface adsorption become dominated by entropy contributions. These experimental observations are compared to theoretical models briefly described below.

Theoretical treatment of adsorption in binary liquids applied in this work are based on the lattice model: a fraction of total number of near-neighbor atoms located within the same layer is defined as l , while m is the fraction of near-neighbors in each of the two adjacent atomic layers, so that $l + 2m = 1$. In the case of a close-packed lattice $l = 0.5$ and $m = 0.25$. A somewhat different mathematical treatment of Gibbs adsorption developed by Cahn [19] avoids the use of conventional dividing surfaces to define surface excess quantities. However, for liquid metal surfaces the lattice model provides a more physically meaningful description due to the quasi-crystalline nature of surface-induced atomic layering. Theory of surface adsorption proposed by Gibbs [1] assumes that compositions of species A and B in surface monolayer x_{A1} and x_{B1} respectively are different from those in the bulk x_A and x_B . Within this model surface tension of the binary mixture γ_{AB} can be determined from surface tension values of the pure components γ_A and γ_B by balancing out the surface excess free energy and entropy contributions [20]:

$$\begin{aligned} \gamma_{AB} &= \gamma_A + \frac{kT}{a_A} \ln\left(\frac{x_{A1}}{x_A}\right) + \frac{w}{a_A} [lx_{B1}^2 - (l + m)x_A^2] = \\ &= \gamma_B + \frac{kT}{a_B} \ln\left(\frac{x_{B1}}{x_B}\right) + \frac{w}{a_B} [lx_{A1}^2 - (l + m)x_A^2] \quad (5) \end{aligned}$$

Here a_A and a_B are the atomic radii of species A and B respectively, while $w = 2w_{AB} - w_{AA} - w_{BB}$ is the *interaction parameter* defined in terms of A-B, A-A and B-B atomic interaction energies. Since $x_{A1} + x_{B1} = x_A + x_B =$

n	$x_n(\text{Bi})$	$Y(x_n)$	δ_n^E	$Y(\delta_n^E)$	δ_n^T
1	0.92	[0.91, 0.95]	0.49	[0.48, 0.52]	0.47
2	0.24	[0.17, 0.27]	-0.19	[-0.26, -0.17]	-0.23
3	0.53	[0.50, 0.54]	0.10	[0.07, 0.11]	0.12
4	0.43	-	0	-	-0.06

TABLE I: density model parameters x_n and $\delta_n^E = x_n - x$ along with confidence intervals $Y(x_n)$ and $Y(\delta_n^E)$ experimentally obtained from fits using three-layer adsorption model compared to theoretical δ_n^T derived from Gibbs theorem ($n=1$) and extended Prigogine-Defay model ($n=2, 3, 4$).

1, we can simplify Eq. 5 in terms of concentration of only one species: $x_1 = x_{A1}$ and $x = x_A$. Surface tension values of pure Bi and pure Sn extrapolated to $T = 142^\circ\text{C}$ are 398 dyn/cm and 567 dyn/cm, while atomic radii for Bi and Sn are 1.70 \AA and 1.62 \AA respectively [21]. If $\text{Bi}_{43}\text{Sn}_{57}$ is treated as a perfect solution ($w = 0$), Eq. 5 otherwise known as *Gibbs theorem* results in Bi composition of $x_1 = 0.904$ and $\gamma_{AB} = 444 \text{ dyn/cm}$, while assuming a regular solution behavior with $w/kT = 1$ changes these numbers to $x_1 = 0.941$ and $\gamma_{AB} = 432 \text{ dyn/cm}$. This range of x_1 values are in remarkable agreement with experimentally obtained Bi composition in surface monolayer of 0.92 (see Table I), while surface tension values agree well with both experimental data and theoretical calculations [22]. It should not be surprising that adsorption amount within the surface monolayer is only weakly affected by interaction parameter w as it is primarily determined by the difference between surface tensions of the two elemental liquids $\gamma_{Sn} - \gamma_{Bi} = 10.8 \text{ kT}$. Strictly speaking, the results of Gibbs theorem (see Eq. 5) based on surface phase model limited to a single monolayer are correct only for perfect solutions. Prigogine and Defay [23] have provided a correction valid for regular solutions by considering a model that extends perturbation of the composition to the first sub-surface layer. Such treatment provides a more detailed description of surface composition profile while it does not significantly change the surface tension result of Gibbs theorem. Their result can be summarized as:

$$\ln \frac{1 + \delta_2/x}{1 - \delta_2/(1 - x)} - \frac{2w}{kT} \delta_2 - \frac{2wm}{kT} (\delta_1 - 2\delta_2) = 0 \quad (6)$$

Here $\delta_1 = x_1 - x$ and $\delta_2 = x_2 - x$ are the differences between concentration of species A in the first and the second layers x_1 and x_2 respectively and that of the bulk x . For small $|\delta_2| \ll 1$, Eq. 6 can be simplified by expansion series while neglecting δ_2^2 and higher order terms:

$$\delta_2 = \frac{2wmx(1 - x)\delta_1}{kT - 2wx(1 - x)} \quad (7)$$

For nearly perfect solutions ($w/kT \ll 1$) the Eq. 6 results in negligibly small δ_2 : $0 < \delta_2 \ll \delta_1$. On the other hand, for sufficiently large w/kT , δ_2 and δ_1 are of the opposite

signs and δ_2 can become comparable to δ_1 , a prediction qualitatively consistent with demixing observed in this study: for $w/kT \gg 1$ the Eq. 7 can be simplified further: $\delta_2 = -(m/l)\delta_1$. Applying this result to Bi₄₃Sn₅₇ for $m/l \approx 0.5$ and taking into account Gibbs theorem predictions of $x_1 = 0.90$ (or $\delta_1 = 0.47$), we obtain: $\delta_2 = -0.23$, $\delta_3 = 0.12$ and $\delta_4 = -0.06$. These values shown as δ_n^T in Table I agree well with δ_n^E obtained from three-layer model fits. The smallest value of interaction parameter w for which we could find a satisfactory agreement with Prigogine-Defay model by treating m as an adjustable parameter is $w = 2.3 kT$.

While w is expected to be directly related to enthalpy of mixing ΔH_m : $w = \Delta H_m/[x(1-x)]$, in practice bulk thermodynamics parameters often cannot accurately account for surface adsorption phenomena. Several reviews of Gibbs adsorption in organic [24] and metallic [25] mixtures justified treating w as an adjustable parameter and observed significant disagreements between w values empirically derived from surface tension measurements and w calculated from bulk calorimetry. Furthermore, in our recent study of BiIn [12] a value of $w \sim 10kT$ that is much greater than those derived from calorimetry measurements was required to justify the observed 35% Bi concentration in the surface monolayer. A survey of literature also reveals a substantial variation between existing thermodynamic functions of mixing for BiSn alloy - most studies indicate positive ΔH_m with a maximum of $\approx 80 - 140$ J/mol at $x \approx 0.4 - 0.5$ [26, 27, 28, 29] which corresponds to $w/kT \approx 0.10 - 0.17$. Such small value of w/kT implies a nearly perfect solution behavior of BiSn alloy in the bulk and within Prigogine-Defay treatment would result in only very subtle ($\delta_2 \approx 0.006 - 0.010$) deviation from bulk composition in the subsurface layer. Cho and Ochoa [30] observed exothermic enthalpy of mixing $\Delta H_m \approx -180$ J/mol at $x=0.6$, but as argued by Asryan and Mikula [29] their results could have been adversely affected by the presence of SnCl₄ electrolytes. Slight asymmetry of $\Delta H_m(x)$ is attributed [29] to short-range ordering previously reported by x-ray and electron diffraction [31, 32]. Such Bi-Sn pairing in the bulk is likely to be enhanced in the near-surface region as evidenced by surface relaxation recently observed in liquid Sn [8]. While some aspects of the reported effect clearly require further investigation, demixing appears to be next in a quickly growing class of surface-induced ordering phenomena in liquids which already includes layering, relaxation, adsorption and surface freezing.

This work has been supported by the U.S. Department of Energy Grants No. DE-FG02-88-ER45379 and DE-AC02-98CH10886 and U.S.-Israel Binational Science Foundation. Technical support from Binhua Lin, Tim Gruber, Mati Meron and Jeff Gebhardt at ChemMat-CARS Sector 15, principally supported by the National Science Foundation/Department of Energy under grant No. CHE0087817 is greatly appreciated. The Advanced

Photon Source is supported by the U.S. Department of Energy under contract No. W-31-109-Eng-38.

-
- * Electronic address: oleg@xray.harvard.edu
- [1] J. W. Gibbs, R. G. V. Name, W. R. Longley and H. A. Bumstead, *The collected works of J. Willard Gibbs* (Longmans, Green and Co., New York, 1928).
 - [2] K. N. Tu *et al.*, *J. Appl. Phys.* **93**, 1335 (2003); J. Glazer, *Int. Mat. Rev.*, **40**, 65 (1995).
 - [3] J. G. Lee and H. Mori, *Phys. Rev. B* **70**, 144105 (2004).
 - [4] M. J. Regan *et al.*, *Phys. Rev. Lett.* **75**, 2498 (1995).
 - [5] O. M. Magnusson *et al.*, *Phys. Rev. Lett.* **74**, 4444 (1995).
 - [6] H. Tostmann *et al.*, *Phys. Rev. B* **59**, 783 (1999).
 - [7] O. G. Shpyrko *et al.*, *Phys. Rev. B* **67**, 115405 (2003).
 - [8] O. G. Shpyrko *et al.*, *Phys. Rev. B* **70**, 224206 (2004).
 - [9] O. G. Shpyrko *et al.*, *Phys. Rev. B* **69**, 245423 (2004).
 - [10] M. J. Regan *et al.*, *Phys. Rev. B* **55**, 15874 (1997).
 - [11] E. DiMasi *et al.*, *MRS Symposium Series* **590**, 183 (2000).
 - [12] E. DiMasi *et al.*, *Phys. Rev. Lett.* **86**, 1538 (2001).
 - [13] P. Huber *et al.*, *Phys. Rev. Lett.* **89**, 035502 (2002).
 - [14] O. G. Shpyrko, Ph.D. thesis, Harvard University, 2003 (unpublished).
 - [15] E. A. Merritt, *Anomalous Scattering Coefficients*, <http://www.bmsc.washington.edu/scatter/> (1996-2003).
 - [16] G. Evans and R. F. Pettifer, *J. Appl. Cryst.* **34**, 82 (2001); J. J. Hoyt *et al.*, *J. Appl. Cryst.* **17**, 344 (1984).
 - [17] M. Newville, computer code IFEFFIT, (1997-2004).
 - [18] Only very weak correlation between x_1, x_2, x_3 adsorption parameters and $d, \sigma_0, \bar{\sigma}$ layering parameters is found. Most of the uncertainty in determination of adsorption model parameters arises from coupling between x_1, x_2 and x_3
 - [19] J. W. Cahn and J. E. Hilliard, *J. Chem. Phys.* **28**, 258 (1958); J. W. Cahn and A. Novick-Cohen, *J. Stat. Phys.* **76**, 877 (1996).
 - [20] E. A. Guggenheim, *Trans. Faraday Soc.*, **41**, 150 (1945).
 - [21] *CRC Handbook of Chemistry and Physics*, ed. by D. R. Lide, (CRC Press, Boca Raton FL, 1996).
 - [22] S. W. Yoon *et al.*, *Script. Mat.*, **40**, 297 (1999); D. T. Ozniev and K. I. Ibragimov, *Poverkh. Yavl. Rasplavakh* **63**, (1983).
 - [23] R. Defay and I. Prigogine, *Trans. Faraday Soc.* **46**, 199 (1950); R. Defay and I. Prigogine, *Surface Tension and Adsorption*, (Wiley, New York 1966).
 - [24] G. L. Gaines, *Trans. Faraday Soc.* **65**, 2320 (1969).
 - [25] T. P. Hoar and D. A. Melford, *Trans. Faraday Soc.* **53**, 315 (1957).
 - [26] R. Hultgren *et al.*, *Selected Values of the Thermodynamic Properties of Binary Alloys*, (Metals Park, OH, 1973).
 - [27] R. L. Sharkey and M. J. Pool, *Metall. Trans.*, **3**, 1773 (1972).
 - [28] H. Seltz *et al.*, *J. Am. Chem. Soc.* **64**, 1392 (1942).
 - [29] N. A. Asryan and A. Mikula, *Inorg. Mat.* **40**, 386 (2004).
 - [30] S. A. Cho and J. L. Ochoa, *Metall. Mater. Trans. B* **28**, 1081 (1997).
 - [31] A. S. Lashko, *Zh. Fiz. Khim.* **33**, 1730 (1959).
 - [32] S. I. Popel and Yu. I. Maslennikov, *Zh. Fiz. Khim.* **51**, 816 (1977).